Eur. Phys. J. B **69**, 483–489 (2009)
DOI: 10.1140/epjb/e2009-00198-y

THE EUROPEAN PHYSICAL JOURNAL B

Regular Article

Surface of underdoped $YBa_2Cu_3O_{7-\delta}$ as revealed by STM/STS

G. Urbanik[1,2,a], T. Hänke[2], C. Hess[2], B. Büchner[2], A. Ciszewski[1], V. Hinkov[3], C.T. Lin[3], and B. Keimer[3]

[1] Institute of Experimental Physics, University of Wroclaw, 50-204 Wroclaw, Poland
[2] Leibniz-Institute for Solid State and Materials Research, IFW-Dresden, 01171 Dresden, Germany
[3] Max Planck Institute for Solid State Research, Stuttgart, Germany

Received 26 October 2008 / Received in final form 29 March 2009
Published online 9 June 2009 –

Abstract. We performed scanning tunneling microscopy and spectroscopy on untwinned crystals of underdoped $YBa_2Cu_3O_{7-\delta}$ at $\delta = 0.4$. A comprehensive statistical analysis of our topographic data indicates a doping dependent cleaving behavior of this material. We find in particular that at $\delta = 0.4$ the material primarily cleaves in multiples of one unit cell along the *c*-axis with a high corrugation of the topmost layer. Our data suggest that the low temperature cleaving mainly results in a *disruption* of the CuO chain layers involving a redistribution of the layer atoms onto the two cleaving planes. In a few instances, fractional step heights (in terms of the *c*-axis lattice constant) are observed as well. Scanning tunneling spectroscopy reveals that such fractional steps connect surfaces which differ significantly in their tunneling conductance.

PACS. 74.72.-h Cuprate superconductors – 74.72.Bk Y-based cuprates – 68.37.Ef Scanning tunneling microscopy

1 Introduction

Major current experimental activities for disentangling the unsolved issue of the physics of high temperature superconductors (HTSC) focus on comprehensive studies of spin and charge dynamics of these intriguing materials across the electronic phase diagram in order to achieve an integrative description of their electronic properties [1–34]. Through their nature, each of the most commonly applied techniques, namely inelastic neutron scattering (INS) for studying spin fluctuations on the one hand and on the other hand angle resolved photoemission (ARPES) and scanning tunneling spectroscopy (STS) for unraveling the charge structure, often rely on different compounds being optimized for the respective technique. For example, ARPES and STS require excellent, preferably atomically flat surfaces which usually are obtained on easy cleaving compounds such as $Bi_2Sr_2CaCu_2O_{8-\delta}$ [15–27] or $Ca_{2-x}Na_xCuO_2Cl_2$ [33,34]. However, despite the high surface quality of these compounds, the crystallinity of the bulk is reduced as compared to the materials like $YBa_2Cu_3O_{7-\delta}$ or $La_{2-x}Sr_xCuO_4$ which are a preferred choice for INS experiments [1–11]. In order to overcome this disjoint situation, more and more attempts are being made to perform surface sensitive experiments on the latter class of HTSC compounds. ARPES on $YBa_2Cu_3O_{7-\delta}$, for example, yields puzzling data for the electronic structure: the spectra often appear to consist of two components. One component corresponds to a doping level higher than the nominal one whereas another appears to better represent properties of the bulk [29–32,35]. This behavior can be reasonably explained by taking into account that the surface layer of $YBa_2Cu_3O_{7-\delta}$ acquires extra charge if cleaving leads to a bipartite breakage [31]. A good knowledge of the surface topology as it can be obtained from scanning tunneling microscopy (STM) is therefore indispensable for drawing general conclusions from such data. The nature of the exposed surface was discussed ever since surface sensitive techniques were applied for investigating the electronic properties of $YBa_2Cu_3O_{7-\delta}$ [28–32,35–49]. STM/STS studies on this material have been performed successfully both on as grown and on cleaved surfaces close to optimal doping [37–50], where already in early, pioneering experiments on twinned crystals (which were cleaved at low temperature $T \lesssim 40$ K) two different terminations were observed as the topmost layers [37,38]. The common picture that arose from such investigations carried out with atomic resolution suggests that $YBa_2Cu_3O_{7-\delta}$ usually cleaves between the BaO plane and the CuO chains plane [37,46–48]. The majority of such studies focused on twinned crystals in the range of optimal doping to overdoping, where the CuO chain layer contain only a few defects from oxygen deficiency. The development of the cleaving behavior of crystals toward underdoping as well as the nature of the exposed surface is less clear. Here the CuO chain layers become increasingly structurally unstable which could give rise to a profound change in the cleaving behavior. The available STM/STS data for the underdoped regime are

[a] e-mail: gurbanik@ifd.uni.wroc.pl

also very rare. Maki et al. reported a doping dependent charge modulation ($\delta \lesssim 0.35$), which was attributed to the CuO chain layer [51]. Clear-cut information about the primarily exposed surfaces at $\delta = 0.35$ and even lower oxygen doping levels, which recently came more and more into focus in experimental studies is however missing.

In this paper, we present a comprehensive surface study of high quality untwinned crystals of underdoped $YBa_2Cu_3O_{7-\delta}$ at $\delta = 0.4$. In particular, we investigate the nature of the surface which is exposed by cleavage in Ultra-High-Vacuum (UHV) at low temperatures. This was done through a detailed statistical analysis of many topographic images in terms of step heights and the roughness of the occurring terminations. We observe that for ∼95% of all topographic images the surface exhibits highly corrugated terraces being separated by steps with a height of integer multiples of the c lattice constant. Step heights of a fraction of c which are observed in STM studies on highly doped $YBa_2Cu_3O_{7-\delta}$ [37,46–49] are however rarely found in our case (∼5% of all topographic images). We conclude from our findings that the nature of the cleaved surface of underdoped $YBa_2Cu_3O_{7-\delta}$ at $\delta = 0.4$ is radically different from that at higher doping levels with $\delta \approx 0$. Instead of a preferred cleaving between the BaO and the CuO chain layers as reported for the latter and which results in two main terminations, our data show that for $\delta \approx 0.4$ only one main termination exists which most likely originates from the disruption of the CuO chain layer upon cleavage.

2 Experimental

High quality $YBa_2Cu_3O_{6.6}$ crystals, which have previously been used in INS [1] and ARPES [28,31] investigations, were synthesized and detwinned as described in reference [1]. All samples used in the STM measurements showed a sharp transition to superconductivity with $T_c = 61 \pm 1$ K. The STM measurements were performed in ultra high vacuum (UHV) using an Omicron VT-STM equipped with a ^{4}He flow cryostat which allowed us to stabilize the sample temperature T between room temperature and $T \approx 25$ K. The STM tip always stayed close to room temperature. Crystals with a typical size of $1 \times 1 \times 0.5$ mm^3 were glued between the sample holder and a small post using conducting epoxy glue which involved baking in air for one hour at 100 °C. After introducing the crystals into the STM head and cooling down to $T \approx 25$ K the crystals were cleaved at this temperature, which exposed in most cases a clean (001) surface. The base pressure was in the low 10^{-10} mbar range. All measurements were performed within 3–6 h after cleavage in order to prevent contamination of the particularly delicate YBCO surface by residual gases. For all tunneling investigations we used chemically etched W tips which prior to tunneling were cleaned on a gold surface at high tunneling voltage and high scanning speed. The topographic images were recorded with a typical tunneling current $I_t \approx 100$ pA and a bias voltage -1.5 V $< V_g < -1$ V (occupied states). In some cases we recorded maps of the differential conductance (dI_t/dV_g) simultaneously with the topography by superimposing a small modulation voltage ($V_{mod} = 5 \ldots 20$ mV) on the gap voltage and detecting dI_t/dV_g with a Lock-In amplifier.

The measurements were performed on 16 freshly cleaved surfaces achieved on a total of 3 different crystals of $YBa_2Cu_3O_{6.6}$. 84 topographic data sets from different sample areas were obtained and form the basis of the surface analysis described below. All topographic images shown in this paper have been plane-fitted and for better visualization we enhanced the contrast of the STM images by mixing the topographic height with its derivative along the fast scanning direction. The statistical analysis has been performed on the raw topographic data. Note, that no qualitative difference between data measured on different crystals were detected.

3 Results

Figure 1 shows a representative micrometer scale topographic STM image of a freshly cleaved surface of untwinned $YBa_2Cu_3O_{6.6}$. The image clearly reveals well defined terraces which are separated by steps of a height $\Delta z \approx 1.11$ nm which (within a typical error of $\lesssim$10%) fairly agrees with the lattice constant $c = 1.17$ nm [1]. Hence the terraces represent surfaces which are exactly normal to the c-axis of the material. A topographic scan with higher resolution on one of these terraces (Fig. 2) reveals a grain-like morphology of the surface. The grains typically possess a width of ∼1 nm and heights of $0.4 \ldots 1.4$ Å. Such structure occurred in the majority of all freshly cleaved surfaces as shown in Figure 1a. Only in a few cases such a structure could not be resolved due to insufficient tip quality.

∼95% of all topographic images show a qualitatively comparable surface structure as described above. The remaining 5% of our data revealed a different surface. Figure 3 shows a representative example for these cases. The topographic scan clearly reveals surface terminations which possess different corrugations. A line scan over several terraces as depicted in Figure 3b shows steps with a height strongly different from the results as presented in Figure 1. Instead of step heights of strictly one c-axis lattice constant, the line profile is characterized by clean steps of 0.65 nm and 0.5 nm corresponding to 0.56 and 0.43 times the c lattice constant, respectively.

This latter surface characteristics was repeatedly observed during different experimental runs in between which the STM tip was changed and a fresh surface was prepared by cleaving. A tip artifact causing such fractional step heights (in terms of the c lattice constant) therefore appears very unlikely and can even be excluded from the simultaneous observation of step heights with both fractional and integer multiples of c in the same scan as depicted in Figure 4.

In the common view, the cleaving of $YBa_2Cu_3O_{7-\delta}$ as observed by STM results almost exclusively in either BaO or CuO chain planes as the topmost layer [37,46–48,51]. For such a cleaving characteristics one would expect not only "one-unit-cell" step heights but also steps a little

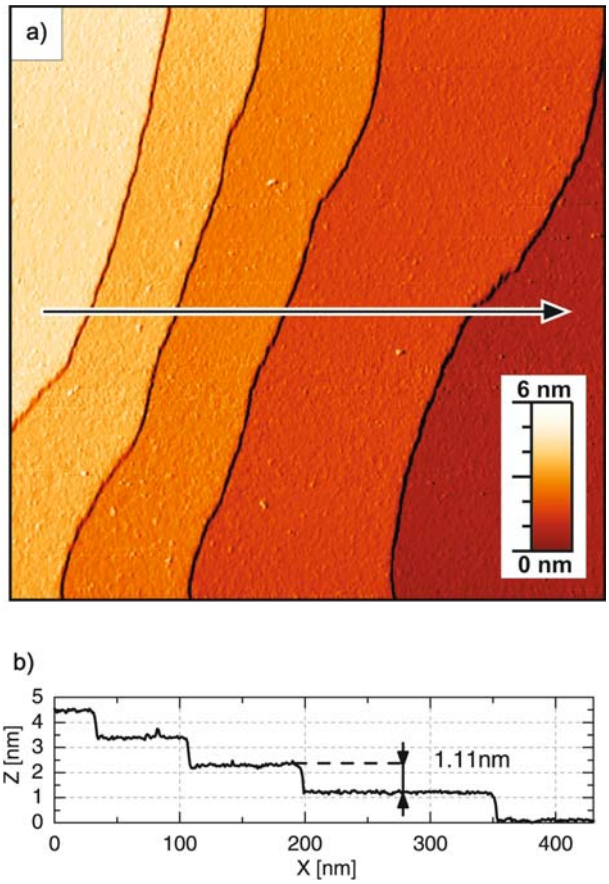

Fig. 1. (Color online) (a) STM topographic image (500 nm × 500 nm) of the cleaved surface of $YBa_2Cu_3O_{6.6}$ at 25 K obtained with $V_g = -1.5$ V and $I_t = 0.1$ nA. The topography consists of flat terraces and steps with the height $\Delta z \approx 1.11$ nm. (b) Line profile from (a) along the indicated arrow.

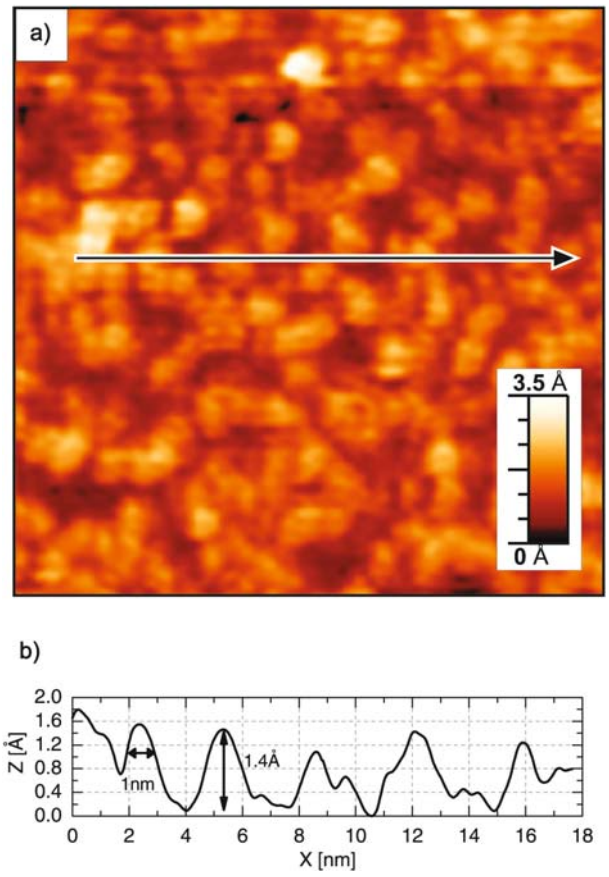

Fig. 2. (Color online) (a) 22 nm × 22 nm zoomed STM image recorded on one terrace shown in Figure 1a. (b) Line profile from a) along the indicated arrow.

bit lower and somewhat higher than this value as well as steps around $0.2c$ [37]. This is a clear consequence of the arrangement of atomic layers in the structure as is illustrated in Figure 5. Since the thickness of the BaO and CuO chain planes is about 0.21 nm each, the observed values of step height smaller than $1c$ should correspond to $\Delta z \approx 1.17$ nm, $\Delta z \approx (1.17 - 0.21)$ nm $= 0.96$ nm, $\Delta z \approx (1.17 + 0.21)$ nm $= 1.38$ nm and $\Delta z \approx 0.21$ nm (corresponding to $1c$, $\sim 0.8c$, $\sim 1.2c$ and $\sim 0.2c$, respectively), when possible influences of the electronic structure on the topographic measurement are ignored (different integrated density of states on different terminations could lead to different tip-sample separation). In fact, probability of finding a "one-unit-cell" step is two times larger since there are two such events possible in the considered cleaving model equal to that of these other values. The data presented here are in clear contradiction to this expectation, since the steps are mostly of the "one-unit-cell"-type and fractional step heights are mostly found to be close to $\Delta z \approx 0.5c$ instead of other values $\sim 0.2c$ and $\sim 0.8c$. Hence, it appears that cleaving of underdoped $YBa_2Cu_3O_{7-\delta}$ does not only occur between the BaO and CuO chain layers. This is corroborated by a detailed analysis of *all* topographic data of our study, which we will discuss below.

In order to quantify the abundance of various step heights in our data we performed a statistical analysis of step heights in our topographic images. More precisely, we measured the total length of step edges with a certain height[1]. The advantage of such a length measurement as compared to the analysis of a z histogram is that the raw topographic data can be analyzed without further data processing (such as error-prone plane fitting). Alternatively one could count steps with a certain height in line profiles (like in Fig. 3) taken from the topographic image. However, such procedure does not always reflect the representative step heights present on the surface. Firstly, measured step heights in a line profile could arise from defects which are usually present in the material (dislocations, etc.). Secondly, by measuring the length of the steps with a certain height we obtain complete statistical

[1] The step edges were detected by searching for extrema within the two-dimensional topographic data and comparing the step height of an identified extremum with the maximum roughness in its vicinity [52]. For each pair of neighboring data points their average step height and their distance is then counted in a histogram. Every pair is taken into account only once.

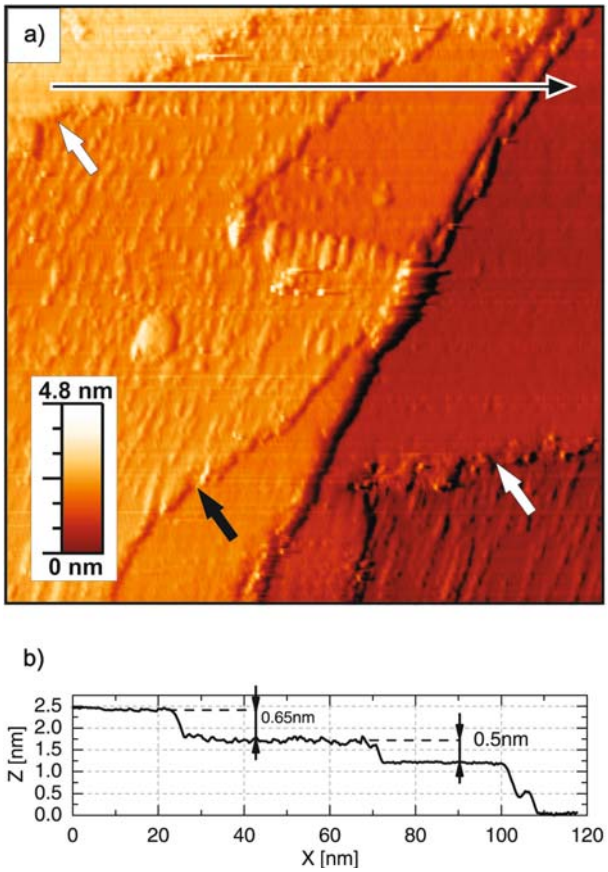

Fig. 3. (Color online) (a) 125 nm × 125 nm topographic image showing the coexistence of flat terraces which are separated by fractional steps (in terms of the c lattice constant). Black and white arrows indicate smaller and higher steps. (b) Line profile from (a) along the indicated arrow.

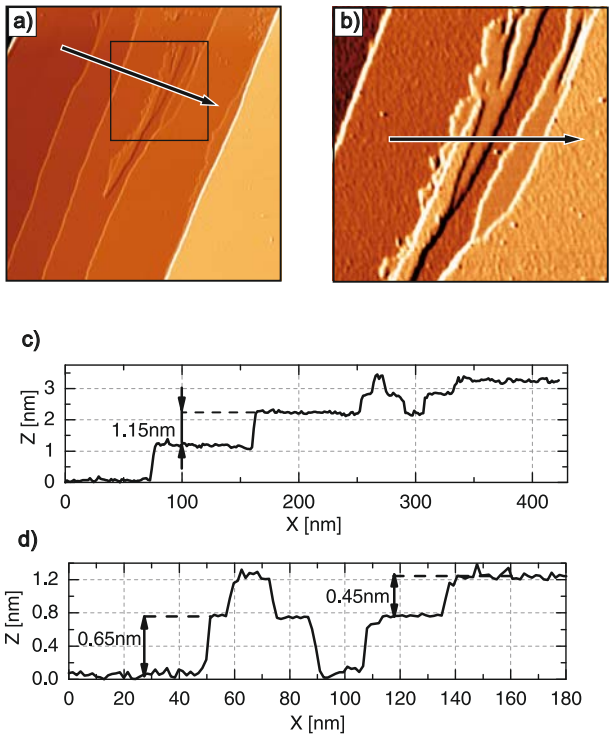

Fig. 4. (Color online) Fractional step heights between different terminations. (a) 700 nm × 700 nm STM topographic image showing mainly one type of termination layer and small areas of another type. (b) Zoomed area from Figure 1a. The different roughness on different layers is visible. (c, d) Line profiles from (a) respectively (b) along the indicated arrows. Two different step heights are observed apart from $\Delta z \approx c$. One with $\Delta z =$ 0.45 nm when going up from a layer with small roughness to one with higher roughness and one with $\Delta z = 0.65$ nm when going up from a layer with higher roughness to one with smaller roughness.

information about the step heights present on the surface which afterwards could be directly compared with a step height measured in a single line profile.

We tested the analysis on the data shown in Figures 1 and 3 in order to verify its sensitivity. Figure 6 shows the result of the step height analysis for the raw data of the topographic image in Figure 1. The analysis clearly reveals a single peak with a Gaussian shape centered at a step height of $\Delta z = 1.11 \pm 0.12$ nm and hence is in good agreement with the c-axis lattice constant of the compound [1]. The fractional step heights which we tentatively detected for example in Figure 3 are also well detected as can be seen from Figure 7 where three peaks are resolved. These correspond to step heights $\Delta z = 0.44 \pm 0.13$ nm, 0.7 ± 0.24 nm, and 1.11 ± 0.14 nm, respectively, and thus are consistent with the steps seen in the line profile of Figure 3b.

Figure 8 shows the results of the step height analysis for the complete set of our data, i.e. it includes *all* individual topographic scans. The data in the figure suggest that the surface of $YBa_2Cu_3O_{6.6}$ exhibits four different step heights, since the curve can be well described by the superposition of four Gaussians. These are centered

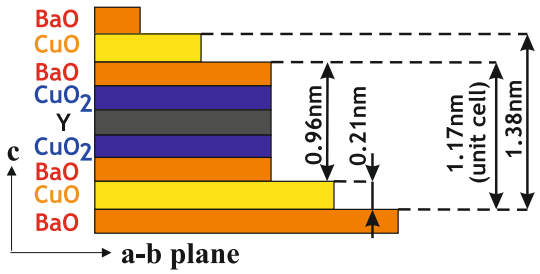

Fig. 5. (Color online) Schematic picture of the $YBa_2Cu_3O_{7-\delta}$ structure highlighting the possible step heights if cleaving occurs between the BaO and CuO chain planes. Given values of the lattice parameters are mean values of the lattice parameters for $YBa_2Cu_3O_{7-\delta}$ at $\delta = 0$ and $\delta = 1$.

at $\Delta z = 1.11 \pm 0.28$ nm, 0.71 ± 0.24 nm, 0.44 ± 0.21 nm, and 0.28 ± 0.09 nm. The first three values for Δz agree very well with Δz detected in the surface topographies shown in Figures 1 and 3. The fourth value suggests the occurrence of steps with $\Delta z = 0.28 \pm 0.09$ nm. However, we could not resolve well defined steps corresponding to this value in any of our topographic scans. It seems

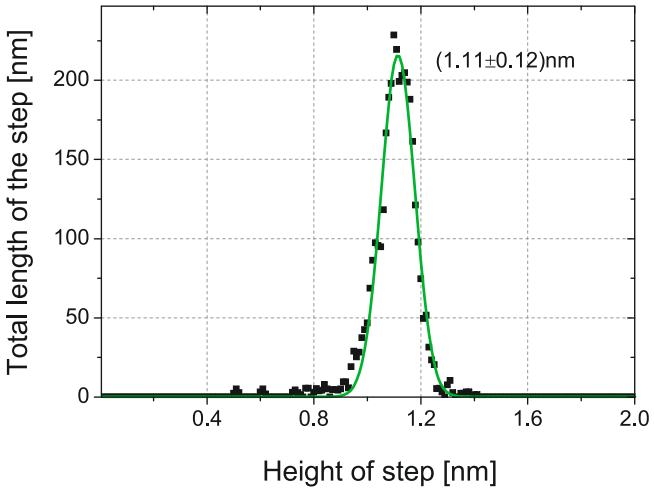

Fig. 6. (Color online) Step height statistics calculated for the raw data of the topographic image in Figure 1. Full symbols denote the statistic events, the solid line represents a Gaussian fit.

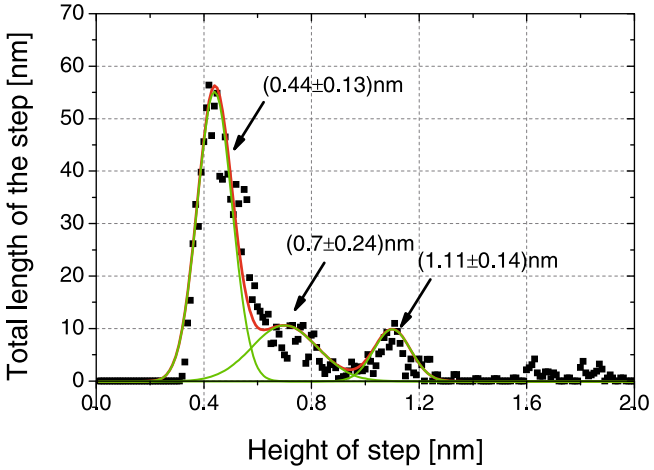

Fig. 7. (Color online) Step height statistics calculated for Figure 3. Full symbols denote the statistic events, the solid lines represent Gaussian fits.

therefore more likely that this value arises from highly corrugated surfaces rather than representing well defined steps. The comparison of the amplitudes of the Gaussians reveals that steps with $\Delta z = c$ have a higher occurrence than steps with a fractional step height. Nevertheless the latter have a significant abundance in our data. Hence, both the integer and the fractional step heights discussed in Figures 1 and 3 are representative for cleaved surfaces of $YBa_2Cu_3O_{6.6}$. We stress, that no indication for a significant abundance of steps with $\Delta z \approx 0.8c$ and $\Delta z \approx 0.2c$ or $\Delta z \approx 1.2c$ are found. This strongly corroborates our afore conjecture that cleaving at this doping level does not occur only and mainly between BaO and CuO.

Note, that the step length which is analyzed in our data does not reflect the *area* of the terminations that are connected with the fractional steps. The ratio of the peak intensities in Figure 8 therefore does not reflect the ratio 95:5 of the two typical surface topographies as discussed above. This method is however very sensitive for detecting steps which form the boundary of terraces with a very small surface area. The detection of such areas is not straightforward in a usual height histogram which would require accurate plane fitting.

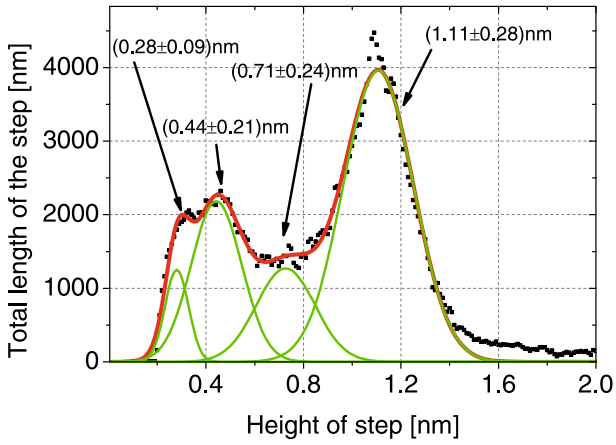

Fig. 8. (Color online) Different step height between the different terminations of all topographic scans. Full symbols denote the statistic events, the solid lines represent Gaussian fits.

Our topographic scans which reveal different surface terminations suggest that steps with a fractional step height usually form the edges of terraces with a lower corrugation as compared to terraces with integer (in terms of c lattice constant) boundaries. We therefore categorized each terrace (in all topographic data) by its roughness and determined the corresponding total areas. We find two major terminations with roughness $S_a = 0.6$ Å and $S_a = 0.4$ Å with an abundance ratio of 19:1. Hence, the data shown in Figure 1 indeed represent the typical cleaving result. The different terminations which are observed in the presence of fractional step heights are very rare. However, if they occur they appear to always involve the same cleaving plane.

We carried out STS measurements on each type of these surface terminations. Figure 9a shows a topographic image with well resolved areas of both types of termination (labeled "A" and "B") as is clearly seen from the line profile depicted in Figure 9c. In this profile, some steps with 1.1 nm, 0.65 nm and 0.55 nm are visible. These correspond to $\sim 1c$, $0.56c$ and $0.47c$. A dI_t/dV_g map at $U_g = 1$ V was recorded simultaneously with the constant current image (cf. Fig. 9b). Apparently the terraces of type A have higher average differential conductance than terraces of type B [2]. A comparison of step heights shown in Figure 9c and those in Figures 3b and 4d suggests that the areas labeled A are areas with a smaller roughness compared to the areas labeled B.

[2] Note that in this scan we were not able to detect any difference in the roughness of these terminations which is probably due to the large scale of the image and/or the tip quality. This reduces the topographic resolution but enhances the spectroscopic signal-to-noise ratio because the tunneling becomes less sensitive to the surface roughness.

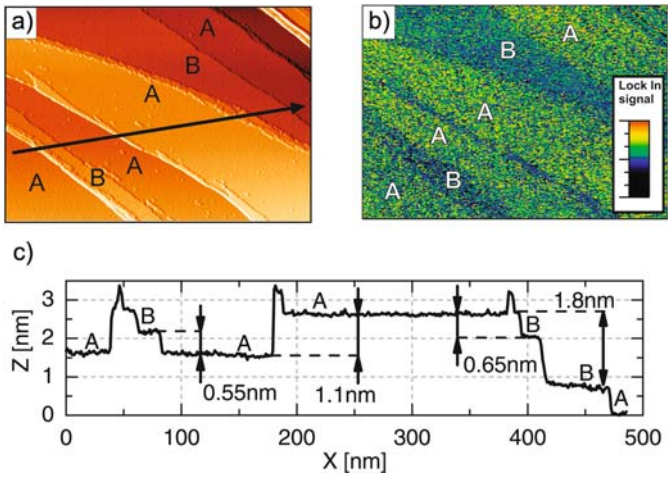

Fig. 9. (Color online) Conductivity of different terminations in $YBa_2Cu_3O_{6.6}$. (a) 500 nm × 350 nm STM topographic image showing different termination layers labeled A and B ($V_g = 1$ V, $I_t = 100$ pA). (b) Differential conductance (d_t/dV_g) map of (a) with $V_g = 1$ V. (c) Line profile from (a) along the indicated arrow.

4 Discussion

The observation of the vast majority of steps being of height $\Delta z = 1c$ implies the cleaving of underdoped $YBa_2Cu_3O_{6.6}$ to take place at one of the two mirror planes of the crystal structure, i.e. either at the Y plane or the CuO chain layer. This is clearly different from cleaving *between* the BaO and CuO layer as it is reported for the optimally doped case [37,39,46–48,51]. Apparently the reduction of the oxygen content introduces a new weak link in the structure which gives rise to this change. The reduced oxygen content within the chain layers naturally produces broken Cu–O–Cu bonds and therefore leads to a weakened internal structure of these planes. At the same time the reduced oxygen content does not lead to a significant structural change at the Y-planes. It is therefore straightforward to conclude that the majority of cleaving events takes place at the CuO chain layers involving a disruption of theses layers.

The identification of the CuO chain layers as the main cleaving plane now implies that the rare but still significant occurrence of fractional steps with $\Delta z \approx 0.5c$ must be related to cleaving close to the Y-layers. In this case one might conclude from the observation of two different Δz close to $0.5c$ (slightly deviating from this value by about ±10%) that the cleaving takes place between the Y and CuO_2 planes. However, in this case we would expect well defined steps with $\Delta z \approx 0.1c$ and $\Delta z \approx 0.9c$ which was not observed. We therefore conclude that the observation of fractional step heights with respect to the CuO chain layers involves the disruption of the Y-layer, i.e. a redistribution of Y between the two cleaved surfaces. The origin of the seemingly different step height between the highly corrugated surface to the lower corrugated surface and vice versa then simply might be a result of different surface conductance of the respective terminations (as is revealed by our spectroscopic data) which leads to somewhat different tip-surface distances.

As already mentioned above, our finding of only one main terminating surface after cleaving underdoped $YBa_2Cu_3O_{7-\delta}$ at $\delta = 0.4$ is radically different from the common picture that cleaving results in BaO and CuO-chain layers as it has been reported for higher oxygen contents [37,39,46–48,51]. This suggests that the cleaving behavior of this material is strongly doping dependent. More precisely, upon reduction of the oxygen content of the material, the topmost exposed surface apparently changes from being either BaO and CuO-chain layers to a single one, which most likely arises from disrupting the CuO chain layer and redistributing the chain material onto the two cleaved counterparts. We point out that this doping dependence of the surface should be considered when surface sensitive spectroscopic techniques are applied to $YBa_2Cu_3O_{7-\delta}$ at various doping levels.

5 Summary

We reported a detailed investigation of the cleaved $YBa_2Cu_3O_{6.6}$ surface using scanning tunneling microscopy and spectroscopy. We have shown that the nature of the exposed surface could be studied indirectly by statistical analysis of the step heights. This simple method detected different step heights present on the cleaved surfaces but mainly steps of multiple of exactly one c lattice constant. Additionally, the analysis revealed that in 95% of cases the surface consists of one type of termination layer. From our findings, we infer a doping dependent cleaving behavior of $YBa_2Cu_3O_{7-\delta}$: the nature of the cleaved surface of underdoped material at $\delta = 0.4$ is radically different from that at higher doping levels with $\delta \approx 0$ which was previously reported [37,39,46–48,51].

It is a pleasure to thank I. Maggio-Aprile and J. Fink for stimulating discussions and A. Narduzzo for proofreading the manuscript. One of the authors (G.U.) would like to thank International Max Planck Research School: Dynamical Processes in Atoms, Molecules and Solids, and Klaus Tschira Foundation for their support. This work has been supported by the Deutsche Forschungsgemeinschaft through the Forschergruppe FOR 538 under Grant No. BU887/4.

References

1. V. Hinkov, S. Pailhès, P. Bourges, Y. Sidis, A. Ivanov, A. Kulakov, C.T. Lin, D.P. Chen, C. Bernhard, B. Keimer, Nature **430**, 650 (2004)
2. V. Hinkov, P. Bourges, S. Pailhès, Y. Sidis, A. Ivanov, C.D. Frost, T.G. Perring, C.T. Lin, D.P. Chen, B. Keimer, Nature Phys. **3**, 780 (2007)
3. V. Hinkov, D. Haug, B. Fauqué, P. Bourges, Y. Sidis, A. Ivanov, C. Bernard, C.T. Lin, B. Keimer, Science **319**, 597 (2008)
4. J. Tranquada, H. Woo, T. Perring, H. Goka, G. Gu, G. Xu, M. Fujita, K. Yamada, Nature **429**, 534 (2004)

5. S.M. Hayden, H.A. Mook, P. Dai, T.G. Perring, F. Dogan, Nature **429**, 531 (2004)
6. D. Reznik, P. Bourges, L. Pintschovius, Y. Endoh, Y. Sidis, T. Masui, S. Tajima, Phys. Rev. Lett. **93**, 207003 (2004)
7. N.B. Christensen, D.F. McMorrow, H.M. Rønnow, B. Lake, S.M. Hayden, G. Aeppli, T.G. Perring, M. Mangkorntong, M. Nohara, H. Tagaki, Phys. Rev. Lett. **93**, 147002 (2004)
8. S.P. Brown, D. Charalambous, E.C. Jones, E.M. Forgan, P.G. Kealey, A. Erb, J. Kohlbrecher, Phys. Rev. Lett. **92**, 067004 (2004)
9. N.B. Christensen, H.M. Rønnow, J. Mesot, R.A. Ewings, N. Momono, M. Oda, M. Ido, M. Enderle, D.F. McMorrow, A.T. Boothroyd, Phys. Rev. Lett. **98**, 197003 (2007)
10. J. Chang, A.P. Schnyder, R. Gilardi, H.M. Rønnow, S. Pailhes, N.B. Christensen, C. Niedermayer, D.F. McMorrow, A. Hiess, A. Stunault et al., Phys. Rev. Lett. **98**, 077004 (2007)
11. S. Pailhès, C. Ulrich, B. Fauqué, V. Hinkov, Y. Sidis, A. Ivanov, C.T. Lin, B. Keimer, P. Bourges, Phys. Rev. Lett. **96**, 257001 (2006)
12. B. Fauqué, Y. Sidis, V. Hinkov, S. Pailhes, C.T. Lin, X. Chaud, P. Bourges, Phys. Rev. Lett. **96**, 197001 (2006)
13. L. Tassini, F. Venturini, Q.-M. Zhang, R. Hackl, N. Kikugawa, T. Fujita, Phys. Rev. Lett. **95**, 117002 (2005)
14. T. Valla, A.V. Fedorov, J. Lee, J.C. Davis, G.D. Gu, Science **314**, 1914 (2006)
15. T. Kondo, R. Khasanov, J. Karpinski, S.M. Kazakov, N.D. Zhigadlo, T. Ohta, H.M. Fretwell, A.D. Palczewski, J.D. Koll, J. Mesot et al., Phys. Rev. Lett. **98**, 157002 (2007)
16. J.F. Douglas, H. Iwasawa, Z. Sun, A.V. Fedorov, M. Ishikado, T. Saitoh, H. Eisaki, H. Bando, T. Iwase, A. Ino et al., Nature **446**, E5 (2007)
17. G.-H. Gweon, T. Sasagawa, S. Zhou, J. Graf, H. Takagi, D.-H. Lee, A. Lanzara, Nature **430**, 187 (2004)
18. V.B. Zabolotnyy, S.V. Borisenko, A.A. Kordyuk, J. Fink, J. Geck, A. Koitzsch, M. Knupfer, B. Büchner, A. Erb, C.T. Lin et al., Phys. Rev. Lett. **96**, 037003 (2006)
19. J.D. Koralek, J.F. Douglas, N.C. Plumb, Z. Sun, A.V. Fedorov, M.M. Murnane, H.C. Kapteyn, S.T. Cundiff, Y. Aiura, K. Oka et al., Phys. Rev. Lett. **96**, 017005 (2006)
20. J. Lee, K. Fujita, K. McElroy, J.A. Slezak, M. Wang, Y. Aiura, H. Bando, M. Ishikado, T. Masui, J.-X. Zhu et al., Nature **442**, 546 (2006)
21. W.S. Lee, I.M. Vishik, K. Tanaka, D.H. Lu, T. Sasagawa, N. Nagaosa, T. Devereaux, Z. Hussain, Z.-X. Shen, Nature **450**, 81 (2007)
22. J.-X. Zhu, K. McElroy, J. Lee, T.P. Devereaux, Q. Si, J.C. Davis, A.V. Balatsky, Phys. Rev. Lett. **97**, 177001 (2006)
23. K. McElroy, J. Lee, J.A. Slezak, D.-H. Lee, H. Eisaki, S. Uchida, J.C. Davis, Science **309**, 1048 (2005)
24. K. McElroy, D.-H. Lee, J.E. Hoffman, K.M. Lang, J. Lee, E.W. Hudson, H. Eisaki, S. Uchida, J.C. Davis, Phys. Rev. Lett. **94**, 197005 (2005)
25. Ø. Fischer, M. Kugler, I. MAggio-Aprile, C. Berthod, Rev. Mod. Phys. **79**, 353 (2005)
26. M. Vershinin, S. Misra, S. Ono, Y. Abe, Y. Ando, A. Yazdani, Science **303** (2004)
27. A.C. Fang, L. Capriotti, D.J. Scalapino, S.A. Kivelson, N. Kaneko, M. Greven, A. Kapitulnik, Phys. Rev. Lett. **96**, 017007 (2006)
28. S.V. Borisenko, A.A. Kordyuk, V. Zabolotnyy, J. Geck, D. Inosov, J.F.A. Koitzch, M. Knupfer, B. Büchner, V. Hinkov, C.T. Lin et al., Phys. Rev. Lett. **96**, 117004 (2006)
29. V.B. Zabolotnyy, S.V. Borisenko, A.A. Kordyuk, J. Geck, D.S. Inosov, A. Koitzsch, J. Fink, M. Knupfer, B. Buchner, S.-L. Drechsler et al., Phys. Rev. B **76**, 064519 (2007)
30. V.B. Zabolotnyy, S.V. Borisenko, A.A. Kordyuk, D.S. Inosov, A. Koitzsch, J. Geck, J. Fink, M. Knupfer, B. Buchner, S.-L. Drechsler et al., Phys. Rev. B **76**, 024502 (2007)
31. V.B. Zabolotnyy, S.V. Borisenko, A.A. Kordyuk, J. Geck, D.S. Inosov, A. Koitzsch, J. Fink, M. Knupfer, B. Büchner, V. Hinkov et al., Physica C **460-462**, 888 (2007)
32. K. Nakayama, T. Sato, K. Terashima, H. Matsui, T. Takahashi, M. Kubota, K. Ono, T. Nishizaki, Y. Takahashi, N. Kobayashi, Phys. Rev. B **75**, 014513 (2007)
33. T. Hanaguri, Y. Kohsaka, J. Davis, C. Lupien, I. Yamada, M. Azuma, M. Takano, K. Ohishi, M. Ono, H. Takagi, Nature Phys. **3**, 865 (2007)
34. Y. Kohsaka, C. Taylor, K. Fujita, A. Schmidt, C. Lupien, T. Hanguri, M. Azuma, M. Takano, H. Eisaki, H. Takagi et al., Science **315**, 1380 (2007)
35. D. Lu, D. Feng, N. Armitage, K. Shen, A. Damascelli, C. Kim, F. Ronning, Z.X. Shen, D. Bonn, R. Liang et al., Phys. Rev. Lett. **86**, 4370 (2001)
36. H. You, U. Welp, G.W. Crabtree, Y. Fang, S.K. Sinha, J.D. Axe, X. Jiang, S.C. Moss, Phys. Rev. B **45**, 5107 (1992)
37. H.L. Edwards, J.T. Markert, A.L. de Lozanne, Phys. Rev. Lett. **69**, 2967 (1992)
38. H.L. Edwards, J.T. Markert, A.L. de Lozanne, J. Vac. Sci. Technol. B **12**, 1886 (1994)
39. H.L. Edwards, A.L. Barr, J.T. Markert, A.L. de Lozanne, Phys. Rev. Lett. **73**, 1154 (1994)
40. H.L. Edwards, D.J. Derro, A.L. Barr, J.T. Markert, A.L. de Lozanne, Phys. Rev. Lett. **75**, 1387 (1995)
41. I. Maggio-Aprile, C. Renner, A. Erb, E. Walker, Ø. Fischer, Phys. Rev. Lett. **75**, 2754 (1995)
42. I. Maggio-Aprile, C. Renner, A. Erb, E. Walker, B. Revaz, J. Genoud, K. Kadowaki, Ø. Fischer, J. Electr. Spectrosc. Relat. Phenom. **109**, 147 (2000)
43. N. Schroeder, R. Böttner, S. Ratz, E. Dietz, U. Gerhardt, T. Wolf, Phys. Rev. B **47**, 5287 (1993)
44. C. Calandra F. Manghi, J. Electron Spectroscopy and Related Phenomena **66**, 453 (1994)
45. K. Kitazawa, H. Sugawara, T. Hasegawa, Physica C **263**, 214 (1996)
46. S.H. Pan, E.W. Hudson, J.C. Davis, Rev. Sci. Instrum. **70**, 1459 (1999)
47. D.J. Derro, E.W. Hudson, K.M. Lang, S.H. Pan, J.C. Davis, J.T. Markert, A.L. de Lozanne, Phys. Rev. Lett. **88**, 097002 (2002)
48. M. Maki, T. Nishizaki, K. Shibata, N. Kobayashi, J. Phys. Soc. Jpn **70**, 1877 (2001)
49. T. Nishizaki, K. Shibata, M. Maki, N. Kobayashi, Physica C **437-438**, 220 (2006)
50. A.V. Narlikar, S.B. Samanta, C. Changkang, H. Yongle, J.W. Hodby, B.M. Wanklyn, J. Cryst. Growth **158**, 248 (1996)
51. M. Maki, T. Nishizaki, K. Shibata, N. Kobayashi, Phys. Rev. B **65**, 140511(R) (2002)
52. B. Jahne, *Digital Image Processing*, 2nd edn. (Springer-Verlag, Berlin Heidelberg, 1993), Vol. 1
53. A.V. Narlikar, S.B. Samanta, Chen Changkang, Hu Yongle, J.W. Hodby, B.M. Wanklyn, J. Cryst. Growth **158**, 248 (1996)